FULL PAPER

BJC

British Journal of Cancer (2014) 111, 1788–1801 | doi: 10.1038/bjc.2014.475

Keywords: MEK kinase; Pancreatic Cancer; MEK162, KRAS

KRAS mutational subtype and copy number predict *in vitro* response of human pancreatic cancer cell lines to MEK inhibition

H Hamidi*[,1], M Lu[1], K Chau[1], L Anderson[1], M Fejzo[1], C Ginther[1], R Linnartz[2], A Zubel[2], D J Slamon[1] and R S Finn*[,1]

[1]*Division of Hematology-Oncology, Department of Medicine, David Geffen School of Medicine, University of California at Los Angeles, Los Angeles, CA 90095, USA and* [2]*Oncology Global Development, Novartis Pharmaceuticals Corporation, One Health Plaza, East Hanover, NJ 07936-1080, USA*

Background: To study the molecular mechanism regulating sensitivity to MEK inhibition in pancreatic cancer cell lines.

Methods: A growth inhibition assay determined sensitivity to MEK162 in a panel of 29 pancreatic cancer cell lines. For the same panel, KRAS mutational status and copy-number variation (CNV) was determine using PCR, array CGH and FISH. Two sensitive and two resistant cell lines were further interrogated for difference in baseline and MEK162-induced gene expression, as well as signal transduction using microarray and western blotting. Cell cycle and apoptosis analysis was measured by flow cytometry.

Results: We report a strong correlation between both specific KRAS mutational subtype and CNV, and sensitivity to MEK inhibition. Cell lines with a KRAS (V12) mutation and KRAS gains or loss ($n=7$) are $\sim$10 times more resistant than those having neither a KRAS (V12) mutation nor KRAS CNV ($n=14$). Significant differences in baseline and MEK162-induced gene expression exist between the sensitive and resistant lines, especially in genes involved in RAS, EGF receptor and PI3K pathways. This was further supported by difference in signal transduction. MEK 162 blocked ERK1/2, as well as inhibited PI3K and S6 and increased p27KIP1 levels in the sensitive lines.

Conclusions: Given the potency of MEK162, it may be a promising new therapy for patients with pancreatic cancer and KRAS mutational subtypes, and CNV may serve as important biomarkers for selecting patients that benefit from MEK-targeting based on these preclinical data.

Pancreatic epithelial cancer is the fourth leading cause of cancer-related death, and 5-year survival is $<7\%$. The incidence rate (44 030 cases per year) is very near the annual death rate (37 660 patients per year) underscoring a lack of effective treatment options for those diagnosed with the disease (Siegel *et al*, 2011). Newer and more effective therapies are definitely needed. Activating mutations in components of the KRAS signalling pathway have been observed in the tumour tissue of all patients with this malignancy, and these alterations are thought to have a major role in pancreatic cancer initiation and/or progression (Jones *et al*, 2008). Ninety percent of patients have activating mutations in *KRAS*, resulting in an abnormal RAS protein that is 'locked' in the activated form. This leads to aberrant activation of the RAS-mediated proliferation and survival signalling pathways. Although effectively targeting KRAS itself has proven challenging to date, targeting the downstream effector MEK1/2, a dual-specific kinase required for activation of ERK1/2, has proven to be effective preclinically in both *in vitro* and *in vivo* preclinical studies (Dudley *et al*, 1995; Sebolt-Leopold *et al*, 1999; Davies *et al*, 2007; Daouti *et al*, 2010). These data led to the development of over 10 small-molecule inhibitors of MEK that are now being studied in preclinical or clinical trials to treat various diseases (reviewed in (Fremin and Meloche, 2010)). Thus far attempts to 'drug' this pathway have also been challenging (Rinehart *et al*, 2004),

*Correspondence: Dr H Hamidi; E-mail: hhamidi@mednet.ucla.edu or Dr RS Finn; E-mail: rfinn@mednet.ucla.edu

Revised 25 June 2014; accepted 31 July 2014; published online 28 August 2014

suggesting either the molecules evaluated to date are not active or that better predictive markers of response are required.

The most prevalent and well-studied mutation in KRAS is at codon 12. The glycine to valine (V12) and glycine to aspartic acid (D12) mutations account for ~90% of codon 12 mutations (Smit *et al*, 1988). Clinical outcome data from pancreatic, colorectal and lung cancers all indicate that some KRAS mutational subtypes have prognostic value evidenced by their association with overall survival (Keohavong *et al*, 1996; Span *et al*, 1996; Kawesha *et al*, 2000). However, no group has assessed them for their use as predictive biomarkers of response to targeted therapy in pancreatic cancer.

In addition, a recent study in colorectal cancer cell lines showed that acquired resistance to the MEK inhibitor selumetinib is mediated by amplification of KRAS (Little *et al*, 2011). Resistance was specific to MEK inhibition as the cells displayed normal sensitivity to cytotoxic drugs including paclitaxel, 5-fluorouracil and cisplatin, however, the predictive value of CNV in KRAS for *de novo* response was not answered.

In this study, we assess the anti-proliferative effects of the MEK inhibitor MEK162 *in vitro*, in a panel of 29 pancreatic cancer cell lines. MEK162 is a novel, orally active, potent, selective, non-ATP-competitive inhibitor of MEK1/2, the dual-specific kinase downstream of both Ras and Raf and required for activation of ERK1/2. We also fully characterised the panel for KRAS mutational and CNV status, and explored whether the type of KRAS codon mutation and/or KRAS CNV are associated with sensitivity to a MEK inhibitor with the objective of determining whether such data could serve to identify biomarkers for selecting patients likely to benefit from MEK162 therapy.

MATERIALS AND METHODS

Cell lines, cell culture and reagents. MEK162 was studied in 29 human pancreatic cancer cell lines *in vitro*. Lines ASPC-1, BxPC-3, Capan-1, Capan-2, CFPAC-1, HPAC, Hs 766T, Hs 700T, MIA PaCa-2, Panc 02.03, Panc 02.13, Panc 03.27, Panc 04.03, Panc 05.04, Panc 08.13, PANC-1, Panc 10.05, PL45, SU.86.86, and SW1990 were obtained from ATCC (American Type Culture Collection, Rockville, MD, USA). Lines DAN-G, HUP-T3, HUP-T4, PATU-8902, PATU-8988S, PATU-8988T and YAPC were obtained from DSMZ (Deutsche Sammlung von Mikroorganismen und Zellkulturen GmbH, Braunschweig,Germany). The line MUTJ was a gift from the Arizona Cancer Center and PSN-1 was obtained from Japan.

Cells were cultured in DMEM, RPMI (Cellgro, Manassas, VA, USA), L-15, or IMDM media according to the manufacture's protocol, supplemented with 10% heat-inactivated fetal bovine serum, 2 mM l^{-1} glutamine and 1% antibiotic–antimycotic solution (Gibco/Invitrogen, Carlsbad, CA, USA). Before any experiments were performed, all cell lines were screened for mycoplasma using previously established methods (Kobayashi *et al*, 2005). Mitochondrial DNA regions of each cell line were also sequenced to confirm individuality using previously established methods (Lee *et al*, 2005).

Proliferation assays. Cells were seeded in duplicate in 24-well plates at densities of 10 000 cells per well. Cells were treated 24 h after initial seeding. MEK162 was added at 10 μM with 10-fold dilutions over six dilutions (ranging from 10 μM to 0.0001 μM). At the time of treatment, one set of untreated cells was collected via trypsinisation and placed in isotone solution for immediate counting using a Coulter-Z1 particle counter (Beckman Coulter Inc., Fullerton, CA, USA). The remaining wells were counted 6 days after seeding. Growth inhibition was calculated by percent generational inhibition (Ather *et al*, 2013). All growth inhibition experiments were performed at least twice.

The combination index (CI) was calculated using the Chou–Talalay method (Chou, 2008). Data were analysed using the Calcusyn software (Biosoft, Cambridge UK) to score synergistic relationships for combination treatments. $CI < 1$, $CI = 1$, and $CI > 1$ indicate synergistic, additive, and antagonistic effects, respectively.

Transfection of synthetic small interfering RNA. Kras (S7939), p27KIP (s2838) and Negative Control No.1 Silencer Select Validated siRNAs were purchased from Life Technologies (Grand Island, NY, USA). YAPC, MIAPACA2, and PANC0203 cells were transfected with the respective siRNAs using Lipofectamine RNAiMAX Transfection (Life Technologies) Reagent using the manufactures protocol. The next day, cells with treated with control, 100 nM and 500 nM of MEK162. Two days after treatment, cells were collected for analysis. There were a total of 15 K cells plated per well in the 24-well plates.

KRAS mutation analysis. Aliquots of each cell line were collected from culture, washed in PBS and then pelleted. Genomic DNA was extracted and purified using the DNeasy Blood & Tissue Kit (Qiagen, Germantown, MD, USA). PCR for exon 1 of KRAS was performed according to previously established methods (Neumann *et al*, 2009). Primers were synthesised by Invitrogen. After the PCR procedure, products were purified using the QiaQuick PCR Purification Kit (Qiagen) to remove unwanted constituents, such as primer-dimers. All sequencing was performed by the UCLA Genotyping and Sequencing Core utilising a 3730 capillary automated sequencer (Applied Biosystems, Foster City, CA, USA) using the forward primer and reverse primer for each product. Sequences were analysed using the Applied Biosystems System Scanner Software and compared with wild-type sequences obtained from the NCBI Entrez Gene database (Bethesda, MD, USA).

KRAS forward primer: 5′-GTGGAGTATTTGATAGTGTATT AAC-3′

KRAS reverse primer: 5′-TGTATCAAAGAATGGTCCTGCA-3′.

DNA isolation and oligonucleotide array comparative genomic hybridisation (aCGH) analysis. Extraction of genomic DNA was performed from frozen cell pellets using the DNeasy Blood and Tissue Kit (Qiagen, Valencia, CA, USA) according to the manufacturer's instructions. Agilent (Santa Clara, CA, USA) 105 K oligo aCGH was performed as described (Konecny *et al*, 2011).

Fluorescence *in situ* hybridisation (FISH). Copy number of the *KRAS* gene was assessed using FISH in 29 pancreatic cancer cell lines. Briefly, cells in culture were collected with trypsin and subjected to 0.67 M KCL hypotonic solution Then the cells were fixed in a 3 : 1 methanol:acetic acid solution. Preparation of samples, hybridisation and microscopy were performed using previously established methods (Ather *et al*, 2013). KRAS Texas Red and CEN12q FITC probes were used (Abnova, Walnut, CA, USA), and samples were counterstained with 4′,6-diamidino-2-phenylin-dole (DAPI).

Microarray analysis. Agilent microarray analyses were used to assess baseline gene expression for 25 pancreatic cancer cell lines. Briefly, cells were grown to log phase. RNA was extracted using the RNeasy Kit (Qiagen). Purified RNA was eluted in 30 to 60 μl DEPC water, and the quantity of RNA was measured by spectral analysis using the Nanodrop Spectrophotometer (Thermo Fisher Scientific, Waltham, MA, USA). RNA separation via capillary electrophoresis using the Agilent 2000 Bioanalyzer was conducted to determine RNA quality.

For the baseline arrays, cyanine-5′-UTP-labelled RNA from an individual cell line was compared with a cyanine-3′-UTP-labelled

RNA from a reference pool (consisting of equal amounts of RNA from 29 pancreatic cancer cell lines) on a single slide. For the treatment arrays, cyanine-5′-UTP-labelled RNA from a cell line treated with 100 nM of MEK162 for 24 h was compared with cyanin-3′-labelled RNA from control cells on a single array.

Microarray slides (whole-human genome 4 × 44 K chips) were read using an Agilent Scanner. Calculation of gene expression values was conducted using Agilent Feature Extraction software version 7.5. Extracted data were imported into Rosetta Resolver 5.1 (Ceiba, Boston, MA, USA) to create expression profiles for each individual cell line experiment. ANOVA and cluster analysis was conducted in Resolver. Baseline (GSE) and treatment (GSE 8) array data have been submitted and accepted in the Gene Expression Omnibus repository.

Statistical methods. Baseline gene expression analyses. Twelve cell lines with KRAS (D12) were compared with 10 cell lines with KRAS (V12) mutation using an error-weighted ANOVA with the Rosetta Resolver software on probes with greater than two-fold change and *P*-value <0.01 in at least one experiment. A *P*-value cutoff of 0.01 was used as the significance cutoff. The same method was applied when comparing two sensitive cell lines to two resistant cell lines.

Gene expression changes in response to MEK162. Two sensitive cell lines were compared with two resistant cell lines using an error-weighted ANOVA with the Rosetta Resolver software on probes with greater than two-fold change and *P*-value <0.01 in at least one experiment. A *P*-value cutoff of 0.01 was used as the significance cutoff.

Pathway enrichment analysis. Gene names associated with significant probes were evaluated for pathway enrichment analysis using Panther Gene Ontology (http://www.pantherdb.org/) as previous (Hamidi *et al*, 2011). Those pathways with significant enrichment (*P*-value <0.05) and that we defined as 'detectable' were considered in the figures. We defined 'detectable' as those pathways with an 'expected' score of at least 1 in all the sets analysed. This would indicate that the gene set associated with that pathway in the Panther database was large enough to evaluate in our data set. Heatmaps representing pathway enrichment were generated using Dchip (Li and Wong, 2001) using –log (*P*-value).

Western blots. Cultured cells in log-phase growth were treated with 100 nM of MEK162 for 10 min, 24 and 48 h. The plates were then washed twice with ice-cold PBS, lysed and collected using mild lysis buffer. Lysates were centrifuged at 10 000 r.p.m. at 4 °C for 10 min to clear insoluble material, and the resulting supernatant was collected and quantified using a bicinchoninic acid assay (Pierce Biochemicals, Rockford, IL, USA). Protein was resolved by SDS–PAGE and transferred to nitrocellulose membranes (Invitrogen). Anti-phospho-AKT (Thr308 cat # 9275), anti-total AKT (cat # 92725), anti-phospho-ERK1/2 (T202/Y204 cat # 9101), anti-total ERK1/2 (cat # 9102), anti-phospho-S6 ribosomal protein (Ser235/236 cat # 2211), anti-total S6 Ribosomal Protein (SG10 cat # 2217), anti-phospho-RB (Ser780 cat # 9307), anti-total RB (cat # 9309), anti-cyclin D1(cat # 2921), anti-phospho cyclin D1 (cat # 2922), anti-phospho-FoxO1(Thr24)/FoxO3a (Thr32) (cat # 9464), anti-p27kip (cat # 2552), anti-beta-actin (cat # 4967), and anti-alpha-tubulin (cat # 2144) antibodies were obtained from Cell Signaling Technologies (Danvers, MA, USA).

Cell cycle analysis. The effects of MEK162 on the cell cycle were investigated using Nim-DAPI staining (NPE Systems, Pembroke Pines, FL, USA). Cells were plated evenly in control and experimental wells and treated 24 h later with 100 nM MEK162 for 24 or 48 h. After aspirating media, cells were washed with PBS, released with trypsin and centrifuged at 3000 r.p.m. for 5 min. The supernatant was removed and 100 μl of the Nim-DAPI solution was added. The solution was gently vortexed and allowed to incubate at room temperature for 5 min before analysis with UV using a Cell Lab Quanta SC flow cytometer (Beckman Coulter, Brea, CA, USA).

RESULTS

Association of specific KRAS mutations with sensitivity to MEK inhibition. Given the known heterogeneity of structural mutations in KRAS, we wanted to assess whether there was any predictive association between these alterations and sensitivity to MEK inhibition. We determined the association of KRAS mutational status at codons 12 and 13 with MEK162 sensitivity, as determined by growth inhibition assays for all 29 lines in the pancreatic cancer cell line panel (Figure 1A). We defined 500 nM as the sensitivity cutoff. There were 15 cell lines with IC_{50} values <500 nM, 14 with an IC_{50} >500 nM and 1 (PATU-8988T) in which the IC_{50} was not achieved at the maximum concentration of 10 μM. These data were then evaluated for any association between sensitivity to MEK inhibition and type of KRAS mutations. There were no detectable mutations at codon13 within the panel. Four cell lines had wild-type KRAS, whereas 25 had a missense mutation at codon 12 (Table 1). Among the 25 of 29 cell lines (86%) with KRAS mutations, 12 had a KRAS (V12) mutation, 10 had a KRAS (D12) mutation, 2 had the KRAS (R12) mutation and 1 had a KRAS (C12) mutation (Table 1). This distribution of KRAS mutational subtypes in the pancreatic cancer cell line panel mimics the frequency of these subtypes seen in tumours from pancreatic cancer patients (Smit *et al*, 1988; Grunewald *et al*, 1989; Nagata *et al*, 1990), indicating that this panel is an appropriate representation of KRAS mutations in the human disease.

Analysing MEK162 response by the type of amino-acid alteration indicated that having a valine KRAS (V12) mutation significantly decreased sensitivity to MEK162 when compared with KRAS (D12) ($P<0.02$) (Figure 1B). In general, a mutation resulting in a polar amino acid at codon 12 will make the cells more sensitive than having a nonpolar amino acid (*P*-value <0.02). The presence or absence of KRAS mutation alone did not predict for sensitivity. We compared the average IC_{50} of the two groups and found no statistical difference between those with mutant *vs* wild-type KRAS ($P=0.5271$) (Figure 1C).

Next, we compared the gene expression profile of the 12 pancreatic cancer cell lines with KRAS (D12) mutation with the 10 with KRAS (V12) mutations. There were 428 probes with significant differences in expression (ANOVA *P*-value <0.01). The dendrogram in Figure 1D shows that these probes cluster in two groups based on whether their expression associated with the KRAS (D12) or KRAS (V12) cell lines. We observed that the 219 probes associated with KRAS (V12) were significantly enriched (*P*-value <0.05) for genes involved in the Wnt, p53, amyloid, presenilin and PI3 kinase pathways (Figure 1E). In addition to genotype-specific gene expression, we compared five KRAS (D12) cells with different sensitivity to MEK162, but similar genotypes (KRAS (D12) and no KRAS copy-number variation). Comparing the resistant Panc0403 and PL-45 cells with the sensitive cell lines PANC05.04, SW1990 and PANC10.05 resulted in 2507 differently expressed probes ((ANOVA *P*-value <0.01), which grouped into two clusters (Figure 1F). The sensitive associated genes are enriched in many growth signalling pathways, including EGF receptor, RAS, FGF, insulin/IGF, and PDFG pathways (Figure 1G).

In addition to structural mutations in KRAS, alterations in copy number are reported for this gene. We assessed whether these might be associated with sensitivity to MEK inhibition. High-resolution oligonucleotide array CGH was performed on the 29 pancreatic cell lines (Table 2). Analysis of these data indicated that only CNVs in KRAS are also associated with sensitivity to

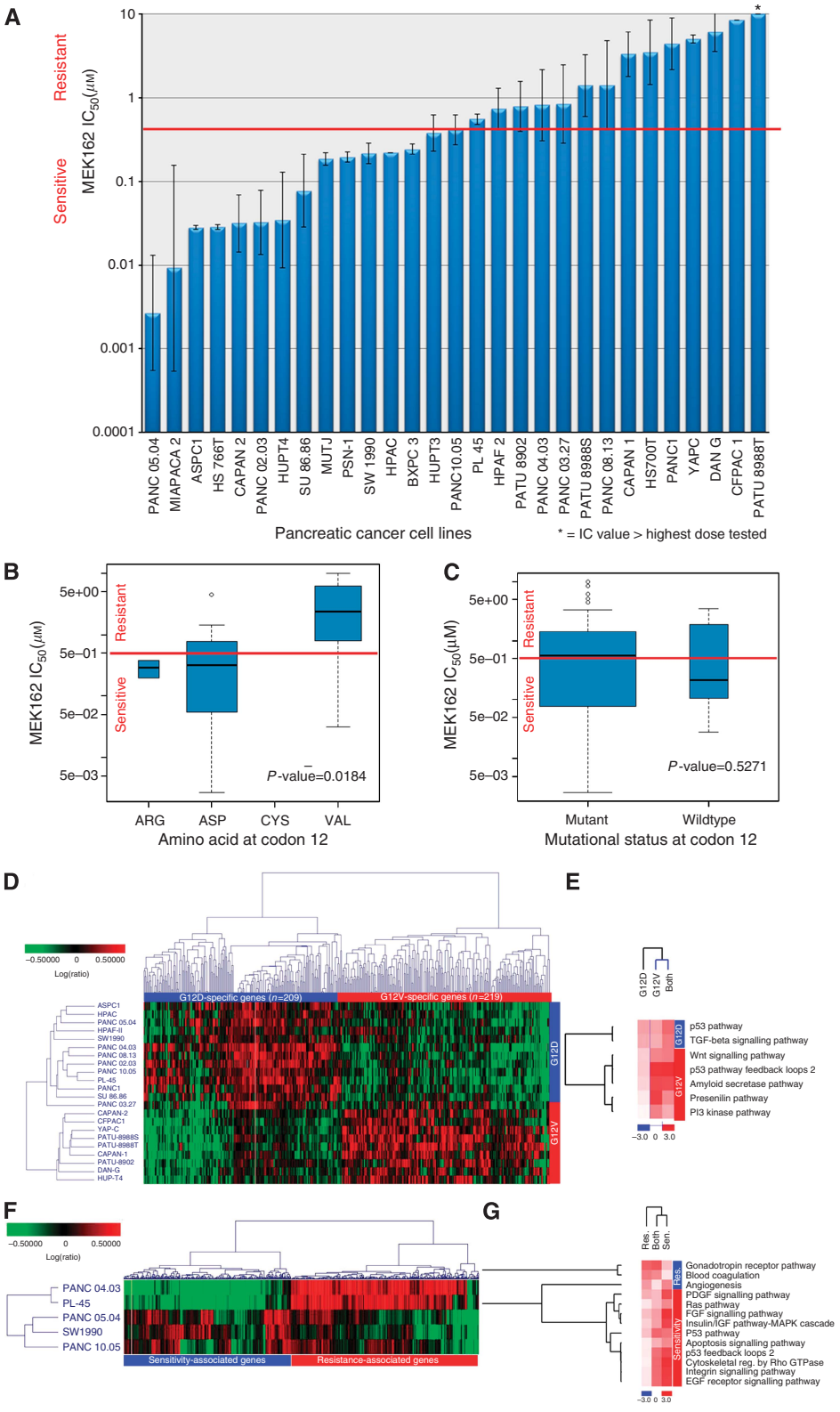

Figure 1. Association of MEK162 sensitivity with specific KRAS mutations in pancreatic cancer cell lines. (**A**) *In vitro* sensitivity of MEK162. Pancreatic cancer cell lines (29) with logIC_{50} represented in μM. Error bars represent 95% confidence intervals. *IC_{50} value was $>10\,\mu$M (highest dose tested). (**B**) Average IC_{50} based on the type of mutant amino acid at KRAS codon 12. Average IC_{50}s of cell lines with KRAS (D12) were compared with average IC_{50}s of cell lines with KRAS (V12) to determine the *P*-value. (**C**) Cell lines with wild-type KRAS ($n=4$) *vs* cell lines with mutant KRAS ($n=25$). The *P*-values were estimated using a Kruskal–Wallis test. Boxplots are average centred IC_{50} values of pancreatic cell lines with given KRAS mutation type. Sensitivity cutoff ($IC_{50}=500$ nM) is marked by a red line. (**D**) Heatmap showing a cluster of 428 probes differentially expressed between the 12 cell lines with KRAS (D12) and 10 cell lines with KRAS (V12) mutations. Probes were identified using ANOVA with a *P*-value cutoff of 0.01. (**E**) Pathway enrichment analysis of the KRAS (D12)- and KRAS (V12)-associated genes. (**F**) Heatmap showing a cluster of 2507 probes differentially expressed between the three sensitive and two resistant cell lines, with KRAS (D12) and normal KRAS copy number. Probes were identified using ANOVA with a *P*-value cutoff of 0.01. (**G**) Pathway enrichment analysis of the sensitivity- and resistance-associated genes. Heatmaps show clustering of pathways that were significantly enriched (*P*-value <0.05) and detectable (expected value >0.5) in the analysed probe sets.

Table 1. IC_{50} values for MEK162 in human 29 pancreatic cancer cell lines, with KRAS copy-number variation, and KRAS codon 12 mutation status, amino-acid type and polarity

Cell lines	MEK162 IC_{50}	S/R	KRAS:CEN (FISH)	KRAS CNV (CGH)	Codon 12 (GGT)	Codon 12 AA	AA polarity
PANC 05.04	0.0027	S	5:5	NC	c.35G>A	ASP	Polar
MIAPACA-2	0.0092	S	4:2	NC	c.34G>T	CYS	Polar
ASPC1	0.0280	S	2:3	NC	c.35G>A	ASP	Polar
HS766T	0.0283	S	2:2	NC	Wild type	GLY	Nonpolar
CAPAN-2	0.0316	S	4:4	NC	c.35G>T	VAL	Nonpolar
PANC 02.03	0.0322	S	3:3	NC	c.35G>A	ASP	Polar
HUP-T4	0.0344	S	3:3	NC	c.35G>T	VAL	Nonpolar
SU 86.86	0.0775	S	AMP:2	AMP	c.35G>A	ASP	Polar
MUT-J	0.1850	S	3:3	NC	Wild type	GLY	Nonpolar
PSN-1	0.1964	S	AMP:3	High AMP	c.34G>C	ARG	Polar
SW1990	0.2159	S	2:2	NC	c.35G>A	ASP	Polar
HPAC	0.2214	S	3:3	NC	c.35G>A	ASP	Polar
BXPC3	0.2420	S	3:3	NC	Wild type	GLY	Nonpolar
HUP-T3	0.3792	S	2:1	NC	c.34G>C	ARG	Polar
PANC 10.05	0.4158	S	4:4	NC	c.35G>A	ASP	Polar
PL-45	0.5585	R	4:4	NC	c.35G>A	ASP	Polar
HPAF-II	0.7352	R	AMP:4	AMP	c.35G>A	ASP	Polar
PATU-8902	0.7844	R	AMP:5	AMP	c.35G>T	VAL	Nonpolar
PANC 04.03	0.8179	R	3:2	NC	c.35G>A	ASP	Polar
PANC 03.27	0.8401	R	5:3	GAIN	c.35G>T	VAL	Nonpolar
PATU-8988S	1.4050	R	2:3	LOH	c.35G>T	VAL	Nonpolar
PANC 08.13	1.4134	R	4: 2	GAIN	c.35G>A	ASP	Polar
CAPAN-1	3.3215	R	2: 2	NC	c.35G>T	VAL	Nonpolar
HS700T	3.4879	R	4:6	NC	wildtype	GLY	Nonpolar
PANC1	4.4236	R	6: 3	AMP	c.35G>A	ASP	Polar
YAP-C	5.0654	R	AMP:3	AMP	c.35G>T	VAL	Nonpolar
DAN-G	6.1748	R	AMP: 2	AMP	c.35G>T	VAL	Nonpolar
CFPAC1	8.5259	R	8:4	GAIN	c.35G>T	VAL	Nonpolar
PATU-8988T	>10	R	2:3	LOSS	c.35G>T	VAL	Nonpolar

Abbreviation: S/R = sensitive/resistant. Bold = significant copy-number variations (copy-number gains (1>log2ratio>0.5), amplification (2>log2ration>1), high amplification (log2ratio>2), hemizygous deletions (−0.8<log2ratio<−1), homozygous deletions (log2ratio<−2)], KRAS mut = KRAS mutations at codon 12.

MEK162. Although the observed CNVs included loss of CDKN2A (Schutte *et al*, 1997) and SMAD4 (Hahn *et al*, 1996) along with MYC amplification (Schleger *et al*, 2002), which have been documented as characteristic of pancreatic cancer, these alterations were not associated with MEK162 sensitivity in this study (Table 2). FISH analysis was used to confirm all observed CNVs (data summarised in Table 2). In the 15 cell lines with IC_{50} <500 nM, defined as sensitive, only 2(13%) had detectable copy-number gains (SU-86.86 and PSN-1 contained amplification), whereas 13(87%) had a normal KRAS copy number. In the 14 cell lines with IC_{50}>500 nM, defined as resistant, 10(71%) had detectable CNVs (gains and losses), whereas only 4(29%) had normal KRAS copy numbers, indicating that cell lines with KRAS CNV have reduced sensitivity to MEK162 (Figure 2A). Moreover, KRAS CNVs were only found in those cell lines with KRAS mutations (Table 2) and this was significant (Fisher's exact test, $P=0.002$). The average IC_{50} in cell lines ($n=12$) with CNVs, either gains or losses, was $\sim 3\,\mu$M as opposed to $0.629\,\mu$M for cell lines ($n=17$) with no change in copy number ($P<0.002$) (Figure 2A). Cell lines with KRAS CNV also had higher levels of KRAS mRNA compared with cell lines with no CNV (Kruskal–Wallis Test, P-value = 0.0041)(Figure 2B). In the two lines with copy-number loss, KRAS was mutated. Previously published data indicate that an absence of the normal allele facilitates transformation by oncogenic KRAS (V12) and has the phenotypic effect of a KRAS (V12) gain (Hegi *et al*, 1994). In our studies, the two cell lines with KRAS loss were as resistant as those with a KRAS gains.

As KRAS (V12) mutations and KRAS CNV both predict resistance to MEK inhibition, we next wanted to evaluate whether they occur together or are mutually exclusive. Figure 2C graphs the average IC_{50} for all the possible KRAS mutational subtype and KRAS copy-number combinations. Clearly the seven cell lines with both KRAS V12 mutation and KRAS CNV are most resistant to MEK162. Figure 2C reduces the possible combination to ± KRAS (V12) and ± KRAS CNV. Cells with a KRAS CNV and KRAS (V12) mutation were less sensitive than cells having neither KRAS CNV nor KRAS (V12) mutations (Kruskal–Wallis test, $P=0.0007$) (Figure 2C). Finally, Figure 2E reduces the combination to three: cell lines with neither KRAS (V12) nor KRAS CNV ($n=14$), cell lines with either a KRAS (V12) or KRAS CNV ($n=8$) and finally cell lines with both a KRAS (V12) and KRAS CNV ($n=7$).

Table 2. Copy-number variation status of KRAS, MYC, CDKN2A and SMAD4 genes in 29 human pancreatic cancer cell lines with MEK162 IC_{50} values

Chr name				chr12	chr8	chr9	chr18
Cytoband				p12.1	q24.21	p21.3	q21.2
Start				25259753	128818041	21958041	46814353
Stop				25259812	128818100	21958099	46814412
Cell line	**IC_{50} (μM)**	**KRAS mut**	S/R	**KRAS**	**MYC**	**CDKN2A**	**SMAD4**
PANC 05.04	0.00	35G>A	S	0.00	0.00	**−2.38**	**−4.15**
MIAPaCa 2	0.01	34G>T	S	0.00	0.53	**−3.15**	0.00
ASPC1	0.03	35G>A	S	0.00	0.50	**−1.46**	**−1.42**
HS-766T	0.03	WT	S	0.00	0.00		**−3.77**
CAPAN-2	0.03	35G>T	S	0.00	0.00	**−0.89**	**−0.85**
PANC 02.03	0.03	35G>A	S	0.00	**0.92**	**−0.86**	**−0.90**
HUP-T4	0.03	35G>T	S	0.00	0.00	**−2.11**	0.00
SU 86.86	0.08	35G>A	S	**1.30**	0.00	**−3.73**	**−1.40**
MUT-J	0.19	WT	S	0.00	0.00	0.00	**−0.91**
PSN-1	0.20	34G>C	S	**2.70**	**5.47**	**−1.37**	**−4.03**
SW1990	0.22	35G>A	S	0.00	0.00	**−2.70**	**−1.35**
HPAC	0.22	35G>A	S	0.00	0.00	0.00	−0.53
BXPC3	0.24	WT	S	0.00	0.00	**−3.19**	**−4.36**
HUP-T3	0.38	34G>C	S	0.00	**2.06**	**−2.20**	0.00
PANC 10.05	0.42	35G>A	S	0.00	**0.85**	0.00	−0.52
PL-45	0.56	35G>A	R	0.00	**0.52**	0.00	**−0.88**
HPAF-2	0.74	35G>A	R	**1.78**	**0.53**	0.00	0.00
PATU 8902	0.78	35G>T	R	**1.27**	**0.82**	0.00	**−0.89**
PANC 04.03	0.82	35G>A	R	0.00	0.00	−0.51	**−1.41**
PANC 03.27	0.84	35G>T	R	**0.56**	0.00	**−2.93**	**−2.73**
PATU 8988S	1.41	35G>T	R	−0.79	0.00	**−1.68**	**−4.57**
PANC 08.13	1.41	35G>A	R	**0.72**	**1.15**	**−2.24**	**−0.78**
CAPAN-1	3.32	35G>T	R	0.00	**1.34**	**−2.93**	−0.53
HS-700T	3.49	WT	R	0.00	**2.32**	0.00	0.00
PANC-1	4.42	35G>A	R	**0.90**	0.00	**−2.95**	−0.50
YAP-C	5.07	35G>T	R	**1.11**	0.00	**−3.33**	**−1.70**
DAN-G	6.18	35G>T	R	**1.55**	0.00	**−3.75**	−0.62
CF-PAC 1	8.53	35G>T	R	**0.51**	**0.88**	**−0.86**	**−4.86**
PATU 8988T	10.00	35G>T	R	−0.53	0.00	−0.61	**−4.52**
P-value				**0.02**	0.715	0.99	1.00

Abbreviation: S/R = sensitive/resistant. Bold = significant copy-number variations (copy-number gains (1 > log2ratio > 0.5), amplification (2 > log2ration > 1), high amplification (log2ratio > 2), hemizygous deletions (−0.8 < log2ratio < −1), homozygous deletions (log2ratio < −2)), KRAS mut = KRAS mutations at codon 12.

Cell lines with a KRAS (V12) mutation and KRAS gains or loss ($n = 7$) have an average IC_{50} of 4.7 μM and are ~10 times more resistant than those having neither a KRAS (V12) mutation nor KRAS CNV ($n = 14$), which had an average $IC_{50} = 0.47$ μM (Figure 2C and E). Similarly, those cell lines with normal KRAS copy number and either a KRAS (D12), KRAS (R12) or KRAS (C12) mutation or no KRAS (V12) mutation are sensitive to MEK162 (Figure 2C–E). These mutational scenarios represented 72% of the pancreatic cancer cell lines investigated. The remainder of the lines had either a KRAS (V12) mutation with normal copies of KRAS or did not have KRAS (V12) mutation and had KRAS copy-number gains. Their sensitivity was intermediate to that of the other groups (Figure 2E).

To assess whether KRAS knockdown resensitises resistant cells to MEK162, we transfected YAPC with negative control and KRAS siRNAs. YAPC is a resistant cell line with a KRAS amplification and KRASV12 mutation. YAPC cells transfected with KRAS siRNA were responsive to 100 nM and 500 nM MEK162 treatment and displayed a significant decrease in cell number after 48 h (Figure 2F). The same effect was not observed in the cells transfected with negative control siRNA.

Finally, to assess whether KRAS CNV variations are associated with sensitivity to other MEK inhibitors in pancreatic cancer cell lines, we compared the Cancer Cell Line Encyclopedia (Barretina *et al*, 2012) IC_{50} data for PD0325901 and AZD6244. KRAS CNV variations were associated with sensitivity to PD0325901 (Figure 2G), but not AZD6244 (data not shown). Pancreatic cancer cell lines were not sensitive to AZD6244, as nearly half (12/25) of the cell lines did not reach IC_{50} in the tested concentration.

Downstream mediators of RAS signalling determine duration of MEK inhibition. To further evaluate sensitivity to MEK162, we selected two sensitive (Panc 02.03 and MIAPACA-2) and two

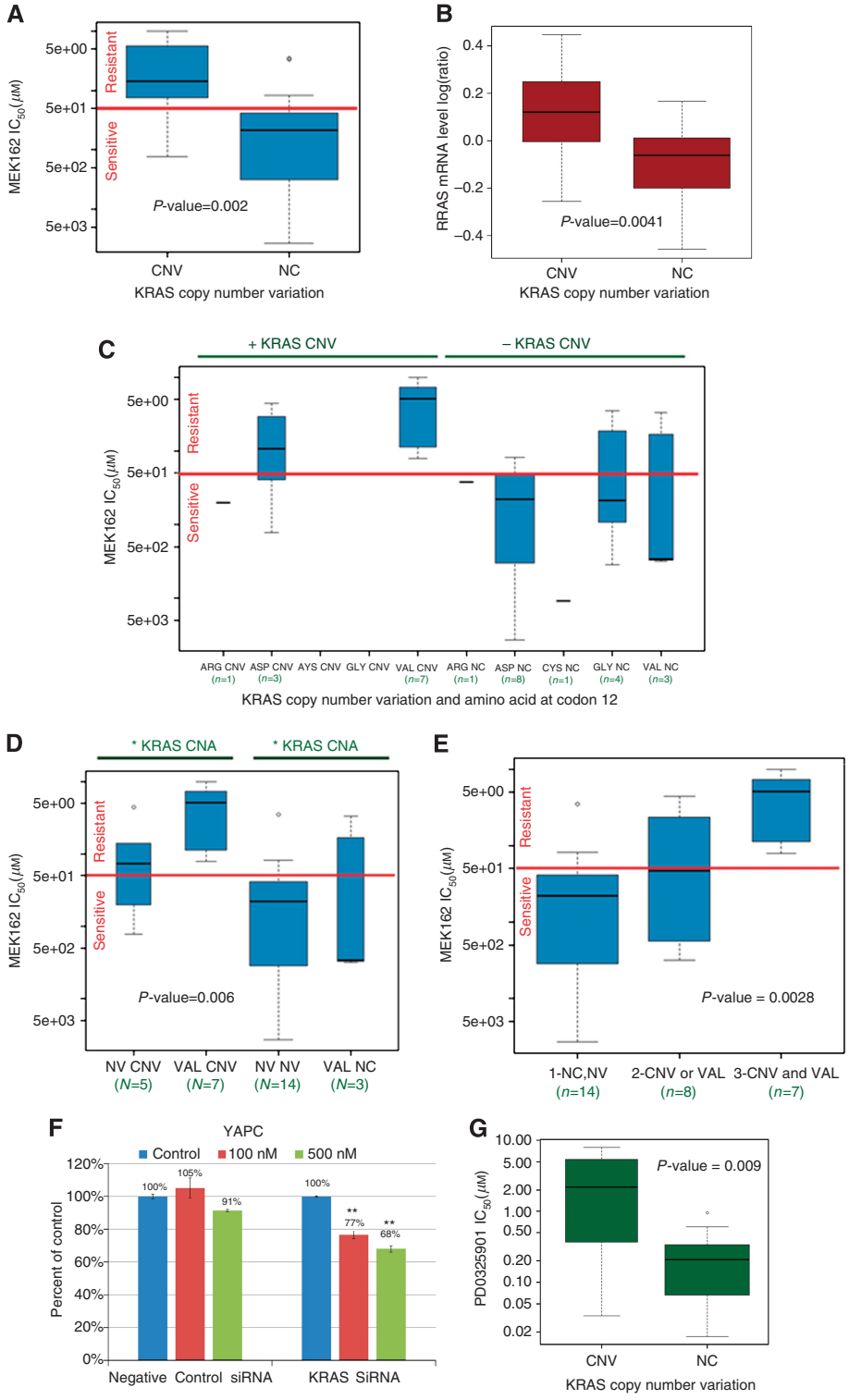

Figure 2. Association of MEK162 sensitivity with KRAS copy-number variation in pancreatic cancer cell lines. Boxplots represent MEK162 IC_{50} (**A**) and KRAS mRNA levels (**B**) of cell lines with normal copies (NC) of KRAS ($n = 17$) *vs* cell lines with copy-number variation (CNV) in KRAS ($n = 12$). (**C**) Cell lines with different combinations of KRAS CNV and mutational subtypes. (**D**) Cell lines with or without KRAS (V12) and with or without KRAS CNV (gains and losses). (**E**) Cell lines with KRAS (V12) and KRAS CNV (CNV and VAL), with KRAS (V12) or KRAS CNV, or without either KRAS (V12) or KRAS CNV. The *P*-values were estimated using a Kruskal–Wallis test. Boxplots are median centred. (**F**) KRAS knockdown resensitises the resistant cell line YAPC to MEK162. Cells transfected with either negative control or KRAS siRNA. The cells were then treated for 48 h with 100 or 500 nM of MEK162 and compared with untreated controls cells. The *P*-values were obtained using a one-sided *t*-test comparing treated cells with controls. ***P*-value < 0.01. (**G**) Sensitivity to the MEK inhibitor PD0325901 is also associated with KRAS CNV. Boxplots of the average PD0325901 IC_{50} of cell lines with normal copies (NC) of KRAS ($n = 15$) *vs* cell lines with CNV in KRAS ($n = 11$). The *P*-values were estimated using a Kruskal–Wallis test. CNV = KRAS gain or loss and NC = normal copies of KRAS.

resistant cell lines (CFPAC1 and YAPC) to analyse changes in gene expression and proteomics.

First, we identified genes' expression patterns associated with MEK162 sensitivity by comparing baseline gene expression patterns. There were 3207 probes with significant differences in expression (ANOVA P-value <0.01). The dendrogram in Figure 3A shows that the 3207 probes cluster in two groups based on whether their expression associated with the sensitive or resistant cell lines. We observed that the 1496 sensitivity-associated probes with high expression in the two sensitive lines and low expression in the resistant lines (Figure 3A) were enriched in genes associated with the EGF receptor pathway, as well as the ubiquitin proteasome and integrin pathways (Figure 3B). MEK inhibition is essentially targeting the EGF receptor signalling pathway and those cell lines whose growth is more dependent on this target pathway, as indicate by higher expression of genes associated with the pathway would be more sensitive. The resistant cell lines are probably more dependent on parallel growth signalling pathways. We observed that the 1711 resistance-associated probes (Figure 3A) were enriched in the Ras pathway as well as the PDGF, cadherin, PI3 kinase, and insulin/IGF pathway (Figure 3B). These alternate growth signalling pathways may compensate for MEK inhibition of the MAPK pathway. Genes associated with the RAS, EGF and PI3K pathways show differential expression based on the sensitivity of the four cell lines (Figure 3C).

In addition to assessing baseline gene expression, we also showed that MEK162-induced gene expression is also correlated with sensitivity to MEK162. There were 1246 probes that were differentially expressed (ANOVA P-value <0.01) between the two sensitive and two resistant cell lines. This indicated that the baseline gene expression difference noted previously results in major differences in how the cells respond to MEK inhibition.

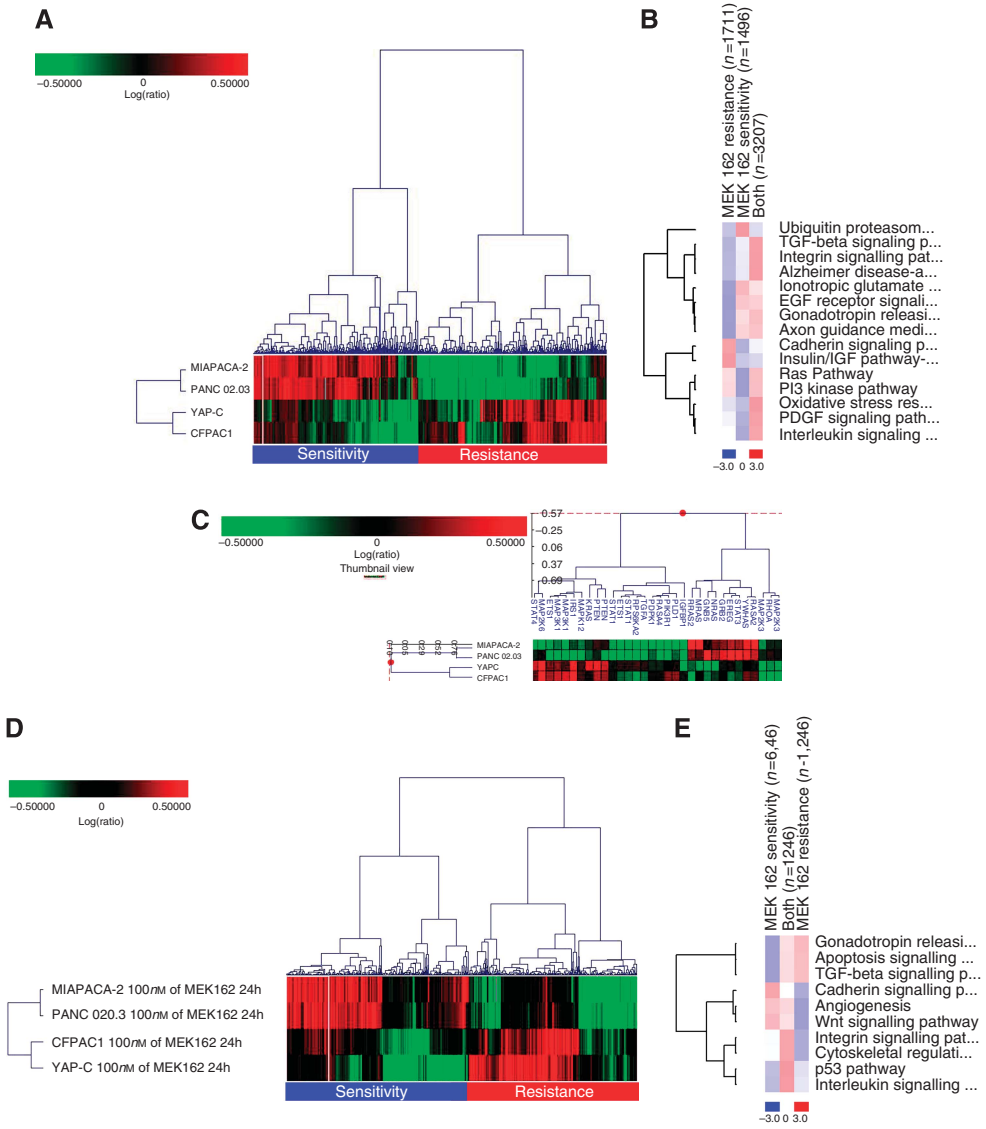

Figure 3. Gene expression analysis of MEK162-sensitive and -resistant pancreatic cancer cell lines. (**A**) Baseline gene expression predicts for MEK162 sensitivity. Heatmap showing a cluster of 3207 probes differentially expressed between the two sensitive (PANC 02.03 and MIAPACA-2) and two resistant lines (CFPAC1 and YAPC). Probes were identified using ANOVA with a P-value cutoff of 0.01. (**B**) Pathway enrichment analysis of the sensitivity- and resistance-associated genes. Heatmap shows clustering of pathways that were significantly enriched (P-value <0.05) and detectable (expected value >1) in the 3207 probe list. (**C**) Heatmap showing clustering of the probes associated with the RAS, EGF or PI3K pathways. (**D**) Gene expression changes in response to MEK162 correlate with sensitivity. Heatmaps show clustering of 1246 treatment-associated probes (ANOVA P-value <0.01) (**E**) Pathway enrichment analysis of treatment-associated genes. Heatmap shows clustering pathways that were significantly enriched (P-value <0.05) and detectable (expected value >1) in the 1246 probe list.

The dendrogram in Figure 3D shows that the 1246 probes cluster into two major groups. MEK162 treatment increased the signal from 646 probes in the sensitive lines. The sensitivity-associated probes were enriched for the integrin, wnt and cadherin pathways as well as angiogenesis (Figure 3E). In the resistant cell lines, MEK62 treatment increased the signal of 600 probes. The resistance-associated probes were associated with the TGF-beta and integrin pathways, as well as apoptosis (Figure 3E).

Using western blot analysis, we assessed the effect of MEK162 on signal transduction involving the MAPK, PI3K, and mTOR pathway-associated protein. First, we tested whether MEK162 sensitivity was associated with its ability to inhibit phosphorylation of ERK1 and ERK2, the immediate targets of MEK1/2. Treatment with 100 nM of MEK162 for 10 min inhibited phosphorylation of ERK1 and ERK2(Figure 4A) regardless of the anti-proliferative effect of the drug (Figure 1A), suggesting that sensitivity of cell lines is independent of the ability of MEK162 to solely inhibit MEK signalling to these intermediaries.

To assess whether changes could be detected at longer time points, two sensitive and two resistant lines were treated for 24 and 48 h (Figure 5). At these longer time points, treatment with 100 nM of MEK162 inhibited phosphorylation of ERK1 and ERK2 in the sensitive lines PANC 02.03 and MIAPaCa-2, but not in the resistant lines YAPC and CFAC1 (Figure 5A), suggesting that sensitivity to MEK162 treatment may be dependent on its ability to maintain inhibition of MEK signalling.

It has been shown that RAS activates the PI3K and raf/MEK/ERK signalling pathways and that the PI3K pathway may compensate for loss of raf/MEK/ERK signalling (reviewed in Steelman *et al*, 2011). After treatment with 100 nM MEK162 for 10 min (Figures 3C and 4B), no changes in AKT or S6 phosphorylation were detected. At longer time points, however, (Figure 5B and C), treatment with 100 nM of MEK162 inhibited phosphorylation of AKT in the sensitive line PANC 02.03, but not in MIAPaCa-2 nor in the resistant lines YAPC and CFAC1 (Figure 5B). Additional evaluation of the two sensitive lines demonstrated that PANC 02.03 had high basal levels of phospho-AKT that decreased after treatment with MEK162 (Figure 5B), whereas MIAPaCa-2 had low baseline levels of phospho-AKT that did not change after treatment. In the two resistant lines there was a different pattern. Basal phospho-AKT levels were low in YAPC cells and increased significantly after treatment with MEK162, whereas CFPAC1 cells had high basal phospho-AKT levels that were not affected by MEK162 treatment (Figure 5B). These data suggest that in sensitive lines the ability of MEK162 to maintain inhibition of the MEK pathway depends on blocking PI3K signalling.

S6 ribosomal protein phosphorylation at Ser235 and Ser236 is associated with cell growth and proliferation, and pS6 is the downstream effector protein of the mTOR, AKT and raf/MEK/ERK pathways (Peterson and Schreiber, 1998). Similar to AKT phosphorylation, levels of pS6, and total S6 were not changed after

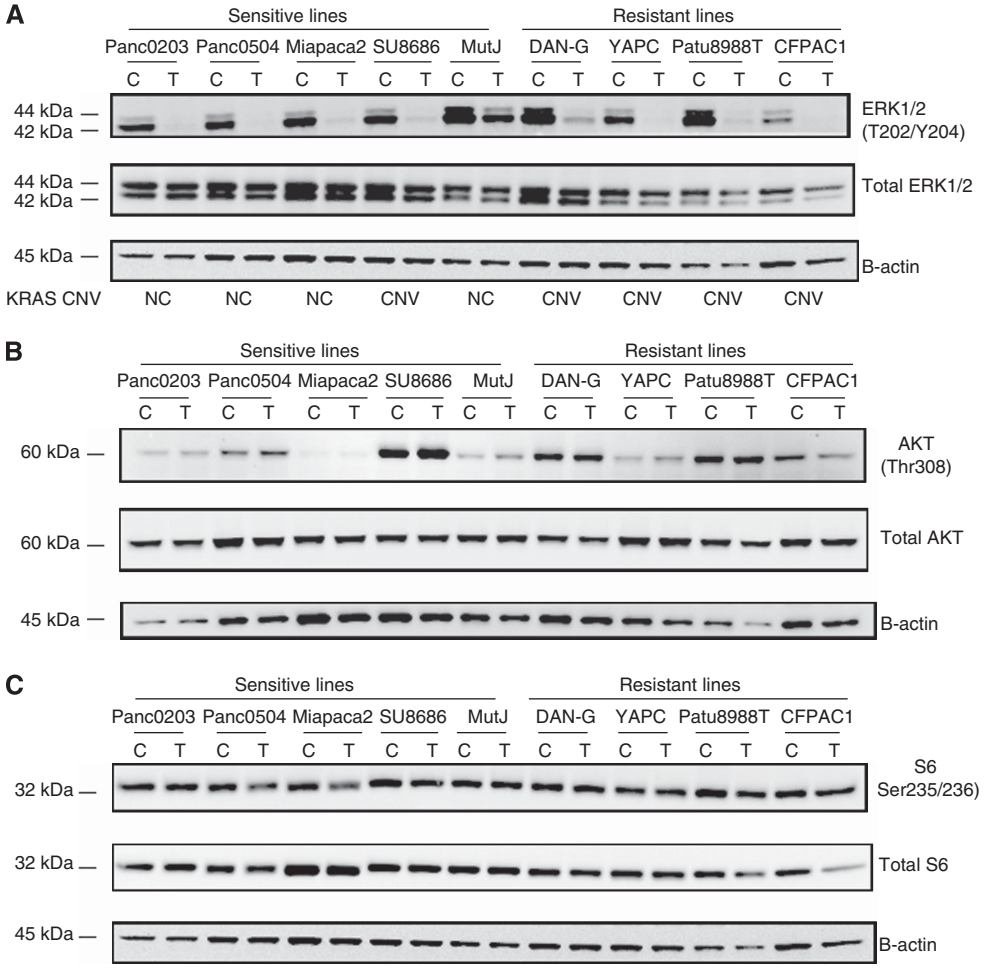

Figure 4. The immediate effect of MEK162 on the MAPK and PI3K pathways in human pancreatic cancer cells. (**A**) MEK162 blocks phosphorylation of ERK1/2. MEK162 has little effect on the phosphorylation of AKT (**B**) and S6 (**C**). Cell lines that were treated with 100 nM MEK162 were compared with untreated control. Sensitive lines = IC_{50} < 1 μM and resistant lines = IC_{50} > 1 μM. Representative western blots are shown. Experiments were done in duplicates.

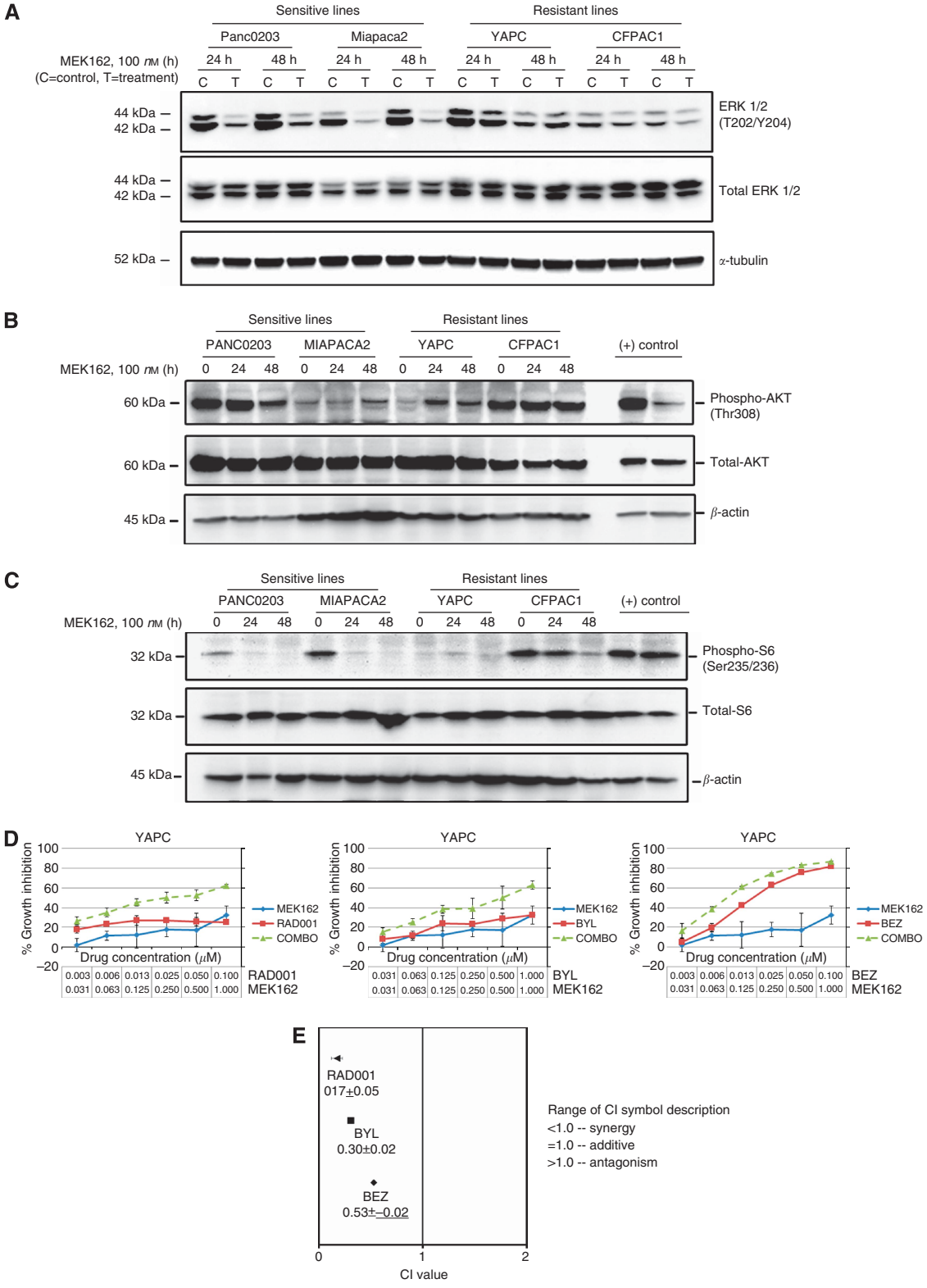

Figure 5. The effect of MEK162 on the MAPK and PI3K pathways in human pancreatic cancer cell lines treated with 100 nM of MEK162 for 24 and 48 h. MEK162 treatment blocks phosphorylation of ERK1/2 (**A**), AKT (**B**) and S6 (**C**) in the sensitive lines and not the resistant lines. Representative western blots are shown. Experiments were done in duplicates. (**D**) The combination of MEK162 with either the mTOR inhibitor RAD001, the PI3K inhibitor BYL or the PI3K/mTOR inhibitor BEZ are synergistic. YAPC cells were plated at 105 cells per well and treated with MEK162 alone, either RAD001, BYL or BEZ alone and in combination. The combination treatment resulted in an increased growth inhibition *in vitro*. Error bars represent s.e.m. (**E**) Mean CI were calculated using Calcusyn software and synergistic values are reported. Error bars represent s.e.m.

short-term (10 min) treatment with 100 nM of MEK162 in either sensitive or resistant lines (Figure 4C), but prolonged exposure to MEK162 resulted in significant decreases in pS6 levels in sensitive lines (Figure 5C). The resistant cell line YAPC had no detectable basal levels of pS6 and the more prolonged treatment did not cause any change, whereas the CFPAC1 cell line, which has high basal

pS6 levels, showed a noticeable decrease in pS6 after 48 h of exposure to MEK162 (Figure 5C). Low basal levels of pS6 may indicate that proliferation in the YAPC cell line is S6 independent. No noticeable changes in total AKT or total S6 were noted when using either short- or long-term MEK162 exposure in any tested cell lines.

We also assessed the contribution of these downstream signalling pathways to MEK162 resistance using pharmacological inhibitors. The resistant cell line YAPC was treated with the mTOR inhibitor RAD001, the PI3K inhibitor BYL or the PI3K/mTOR inhibitor BEZ alone or in combination with MEK162 (Figure 5D). MEK162 in combination with any of these inhibitors was more effective then treatment with any single agent alone. MEK162 displayed strongest synergy with the mTOR inhibitor RAD001(Figure 5E).

MEK inhibition promotes cell cycle arrest via RB hyperphosphorylation and p27KIP1 expression. MEK162 induced cell cycle arrest, but not apoptosis, in the pancreatic cancer cell lines tested (apoptosis data not shown). Treatment with 100 nM of MEK162 significantly increased percent of cells in G0/G1 in sensitive, but not resistant cell lines (Figure 6A). To determine how MEK162 may induce cell cycle arrest, western blot analyses were performed on key cell cycle-associated proteins. Although ERK1/2 signalling is known to promote cell cycle progression by increasing the amount of cyclin-D, we did not observe any association between cyclin-D1 levels and MEK162 sensitivity (Figure 6B). Phosphorylation of cyclin-D1 at Thr286 is associated with ubiquitin-mediated proteolysis (Shao *et al*, 2000), and we observed an accumulation of phospho-cyclin-D1 in the resistant but not sensitive lines; however, treatment with 100 nM of MEK162 did not change levels of phospho cyclin-D1 in any of the four tested cell lines. In contrast, we did observe a correlation between RB levels (both total RB and phospho-RB) and MEK162 sensitivity. Hyperphosphorylation of RB is a necessary step to progress through the G1/S checkpoint in ERK1/2-mediated cell cycle progression. These data indicate an association between MEK inhibition and hypophosphorylation of RB in the two sensitive, but not the two resistant cell lines (Figure 6B). This observation is consistent with MEK162-induced cell cycle arrest in sensitive lines. A concurrent decrease in total RB was also noted in association with MEK162 sensitivity (Figure 6B).

We also assessed the levels of the cell cycle inhibitor p27KIP1 (Figure 6C), which is associated with MEK inhibition (Yip-Schneider and Schmidt, 2003). Activated KRAS and Akt phosphorylation of p27KIP1 leads to the translocation of p27KIP1 from the nucleus to the cytoplasm, where it becomes degraded, resulting in cell cycle progression (Liu *et al*, 2000; Fujita *et al*, 2002; Kamura *et al*, 2004; Besson *et al*, 2006).

In the two sensitive lines with low basal levels of p27KIP1, treatment with 100 nM of MEK162 increased p27KIP1 protein levels at both the 24 and 48 h time points (Figure 6B) and is in juxtaposition with data showing that the two MEK162-resistant lines that had low basal levels of p27KIP1, and the MEK162 induction of p27KIP1 is inhibited. To assess whether p27KIP1 knockdown desensitised the sensitive cell line PANC0203 and MIAPACA2 to MEK162, both cell lines were transfected with p27KIP1 or negative control siRNA and treated with either control or 100 nM of MEK162 for 48 h. PANC0203 and MIAPACA transfected with negative control siRNA were responsive to 100 nM of MEK162 and displayed a significant decrease in cell number after 48 h (Figure 6D). The same effect was not observed in the cells transfected with p27KIP1 siRNA. This result provides evidence that p27KIP1 has a critical role in MEK162-mediated cell cycle arrest.

Alteration of p27KIP1 levels has been associated with PI3K signalling via Akt, which inhibits p27KIP1 protein levels (Yang *et al*, 2012) and blocks transcription of p27KIP1 by phosphorylating forkhead transcription factors (Medema *et al*, 2000). Furthermore, activation of forkhead transcription factor may mediate the antiproliferative effects of MEK inhibitors (Yang *et al*, 2010). We did not observe an association between the levels of phospho-FOXO3a (Thr 32) and FOXO1(Thr24) levels and p27KIP1 levels (Figure 6C). We also did not observe an association between levels of phospho-FOXO3a (Thr 32) and FOXO1(Thr24) and sensitivity to MEK162(Figure 6C).

DISCUSSION

In this study, the biologic and molecular effects of MEK inhibition in 29 human pancreatic cancer cell lines were evaluated using the novel MEK162 inhibitor. The resulting data demonstrate MEK162 sensitivity was associated with KRAS mutational subtypes and CNVs in the pancreatic cancer cell lines. Cells sensitive to MEK162 have a greater degree of G0/G1 arrest, reduced phosphorylation of RB and increased levels of p27KIP1 after exposure. They also displayed differences in both baseline and MEK162-induced gene expression.

KRAS mutations and subsequent hyperactivation of RAS signalling pathway is a molecular hallmark of pancreatic cancer. As a result, this presumptive pathogenic molecular alteration could potentially be targeted using an inhibitor of a critical downstream component, that is, MEK. Our data indicate that MEK162 is an effective small-molecule inhibitor of MEK signalling significantly reducing phosphorylation of ERK1 and ERK2 in pancreatic cancer cell lines, regardless of the growth inhibitoryeffects of the drug. The current study indicates that prolonged inhibition of MEK signalling is critical in conferring sensitivity to MEK162 and this prolonged inhibition is absent in resistant lines. These data indicate that the apparent molecular heterogeneity of pancreatic cancer requires a more complex analysis of the RAS signalling pathway rather than simply assessing for the presence or absence of KRAS mutations.

Our data suggest that patients with normal KRAS copy number and either a KRAS (D12), KRAS (R12) or KRAS (C12) mutation may be most sensitive to MEK162. These mutational scenarios represent 48% of pancreatic cancer cells tested. Moreover, patients with KRAS (D12) mutation have lower survival rates than those with KRAS (V12) mutation (Kawesha *et al*, 2000), and our data indicate that MEK162 might be most effective in this subgroup of pancreatic cancer.

In addition, the current findings emphasise the importance of testing for the nature of specific KRAS mutational status. KRAS mutations were originally detected in lung cancer (Rodenhuis *et al*, 1987) and since then have been assessed as a potential marker of survival in colorectal, ovarian and pancreatic cancers. However, our report is the first to suggest that specific KRAS mutational subtypes can also be used to predict response to targeted therapy.

It is interesting that our baseline gene expression data showed major difference in gene expression between sensitive and resistant cell lines (Figure 3A). This supports the notion that the molecular context of the cell line determines the cell's reaction to inhibitors. Those cell lines with the appropriate molecular circuitry that is reliant on the targeted pathway are more likely to respond. Sensitive cell lines also responded differently to MEK162 than resistant cell lines (Figure 3D). There were over 1200 genes with differential expression in response to MEK162 treatment.

Our findings suggest that cancers harbouring KRAS (V12) and KRAS copy-number variation (both gains and loss) may be less likely to respond to MEK162. These KRAS alterations may lead to sustained PI3K signalling and inhibition of p27KIP1 levels. PI3K signalling via AKT can regulate p27KIP1 levels by inhibiting p27 protein levels (Yang *et al*, 2012). This is a plausible explanation for our findings, as PI3K signalling was found to be either high at

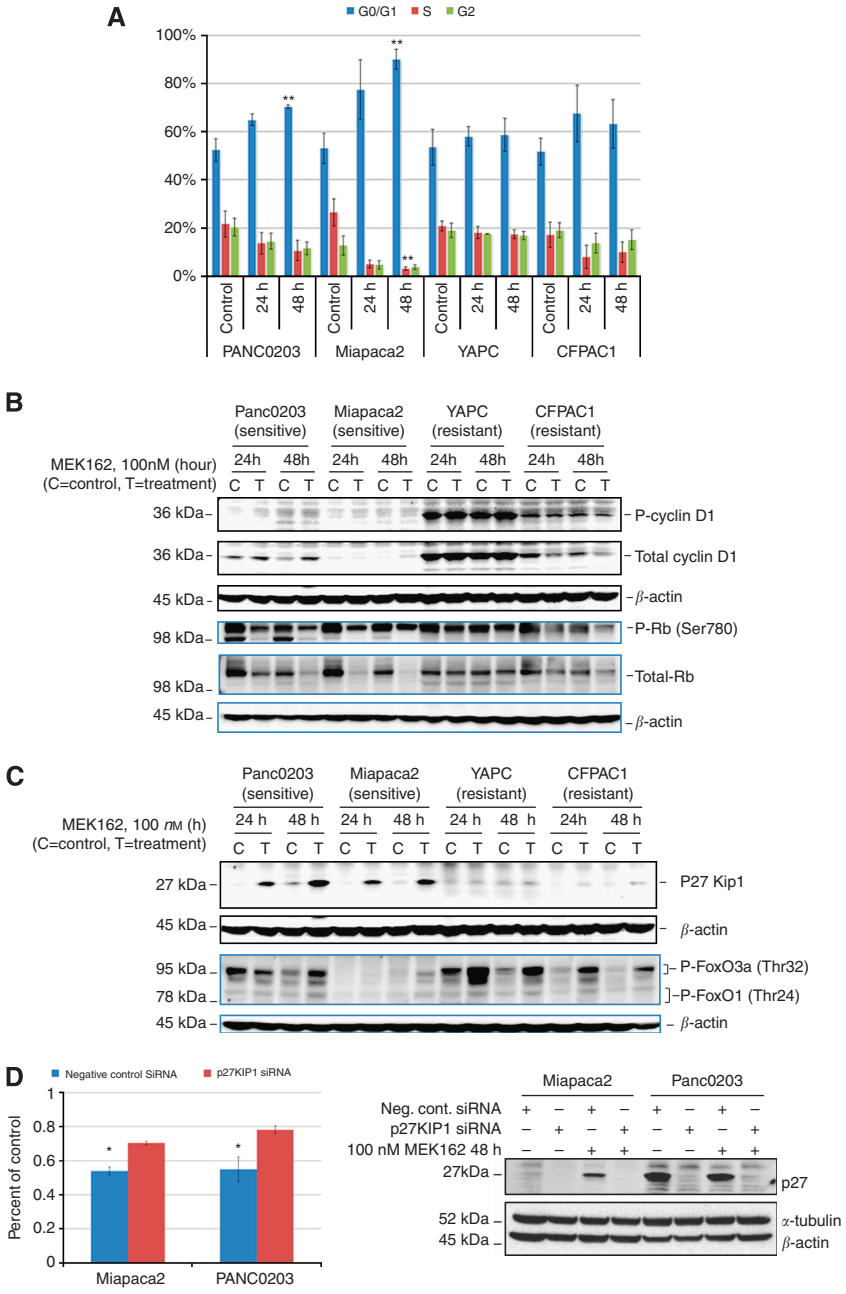

Figure 6. The effect of MEK162 on cell cycle and cell cycle-associated proteins. (**A**) MEK162 induces cell cycle arrest in the sensitive and not the resistant lines. The experiment was performed in triplicate; error bars represent s.d. Treated time points were compared with untreated control and significance was assessed using a *t*-test (**t-test P-value <0.01). (**B**) MEK162 decreased total and phospho RB in the sensitive lines. Total and phosphor D1 levels are greater in the resistant lines. (**C**) MEK162 induces p27KIP1 in the sensitive lines and not the resistant lines and is not associated with the phosphorylation of the forkhead transcription factors FoxO1 and FoxO3a. Cell lines were treated with 100 nM MEK162 for 24 or 48 h and compared with untreated controls. Representative western blots are shown. Experiments were done in duplicates. (**D**) p27KIP knockdown desensitises the sensitive cell lines MIAPACA2 and PANC0203 to MEK162. Cells were transfected with either negative control or p27KIP1 siRNA. The cells were then treated for 48 h with 100 nM of MEK162 and compared with untreated controls cells. The *P*-values were obtained using a one-sided *t*-test comparing treated cells with controls. *P-value <0.05.

baseline or increased in response to MEK162 treatment in MEK162-resistant cell lines (Figure 5B). The resistant line YAPC had low levels of phospho-AKT and the levels increased significantly after treatment with MEK162, whereas the resistant line CFPAC1 had very high basal levels of phospho-AKT and the levels were unaffected by MEK162 treatment. High levels of phospho-AKT may be indicative of active PI3K signalling and could account for inhibition of p27KIP1 in the resistant lines.

Conversely, in the sensitive lines, phospho-AKT levels were either low and remained low with MEK162 treatment, or were high and markedly reduced with MEK162 treatment. This suggests two mechanisms for the role of the PI3K pathway in sensitive cell lines. In some lines it is not very active at baseline, whereas in others, PI3K signalling is active and MEK162 treatment leads to a reduction. Both scenarios may result in relieving PI3K inhibition of p27KIP1 protein levels.

PI3K signalling can also inhibit FOXO-mediated transcription of p27KIP1 by phosphorylating FOXO transcription factors (Medema *et al*, 2000). On the basis on our assessment of phospho-FOXO3a and FOXO1 levels, this hypothesis is not

supported by the data. Phospho-FOXO3a and FOXO1 levels (Figure 6C) did not associate with p27KIP (Figure 6C) nor phospho-AKT levels (Figure 5B).

We defined our sensitivity cutoff at 500 nM. Achievable C_{max} in patients is 466 ng ml^{-1} (Ascierto *et al*, 2013) or about 1 μM and, our conservative cutoff of 500 nM is well within the range of this upper limit. Previous studies of the kinase inhibitor U0126, with MEK inhibitory activity, have demonstrated that sensitivity to this compound is associated with the ability to induce p27KIP1 (Yip-Schneider and Schmidt, 2003; Gysin *et al*, 2005) albeit at doses of 2–10 μmol l^{-1}, which is 100- to 250-fold greater than the concentration of MEK162 used in this study to show the same effect, confirming that MEK162 is a more potent MEK inhibitor.

In summary, using molecularly characterised human pancreatic cancer cell lines, we have generated a hypothesis for patient selection that may be useful in clinical evaluation of MEK inhibition. Clearly, prospective clinical confirmation of this hypothesis will be required, but the preclinical data would support evaluation of such a strategy.

ACKNOWLEDGEMENTS

This work is supported in part by a generous gift from the Bill and Charlene Glikbarg Foundation for Emerging Therapies for Pancreatic Cancer (RSF).

CONFLICT OF INTEREST

The authors declare no conflict of interest. This work is supported in part by a generous gift from the Bill and Charlene Glikbarg Foundation for Emerging Therapies for Pancreatic Cancer (RSF).

REFERENCES

Ascierto PA, Schadendorf D, Berking C, Agarwala SS, van Herpen CM, Queirolo P, Blank CU, Hauschild A, Beck JT, St-Pierre A, Niazi F, Wandel S, Peters M, Zubel A, Dummer R (2013) MEK162 for patients with advanced melanoma harbouring NRAS or Val600 BRAF mutations: a non-randomised, open-label phase 2 study. *Lancet Oncol* **14**(3): 249–256.

Ather F, Hamidi H, Fejzo MS, Letrent S, Finn RS, Kabbinavar F, Head C, Wong SG (2013) Dacomitinib, an irreversible Pan-ErbB inhibitor significantly abrogates growth in head and neck cancer models that exhibit low response to cetuximab. *PLoS One* **8**(2): e56112.

Barretina J, Caponigro G, Stransky N, Venkatesan K, Margolin AA, Kim S, Wilson CJ, Lehar J, Kryukov GV, Sonkin D, Reddy A, Liu M, Murray L, Berger MF, Monahan JE, Morais P, Meltzer J, Korejwa A, Jane-Valbuena J, Mapa FA, Thibault J, Bric-Furlong E, Raman P, Shipway A, Engels IH, Cheng J, Yu GK, Yu J, Aspesi Jr. P, de Silva M, Jagtap K, Jones MD, Wang L, Hatton C, Palescandolo E, Gupta S, Mahan S, Sougnez C, Onofrio RC, Liefeld T, MacConaill L, Winckler W, Reich M, Li N, Mesirov JP, Gabriel SB, Getz G, Ardlie K, Chan V, Myer VE, Weber BL, Porter J, Warmuth M, Finan P, Harris JL, Meyerson M, Golub TR, Morrissey MP, Sellers WR, Schlegel R, Garraway LA (2012) The Cancer Cell Line Encyclopedia enables predictive modelling of anticancer drug sensitivity. *Nature* **483**(7391): 603–607.

Besson A, Gurian-West M, Chen X, Kelly-Spratt KS, Kemp CJ, Roberts JM (2006) A pathway in quiescent cells that controls p27Kip1 stability, subcellular localization, and tumor suppression. *Genes Dev* **20**(1): 47–64.

Chou TC (2008) Preclinical versus clinical drug combination studies. *Leuk Lymphoma* **49**(11): 2059–2080.

Daouti S, Higgins B, Kolinsky K, Packman K, Wang H, Rizzo C, Moliterni J, Huby N, Fotouhi N, Liu M, Goelzer P, Sandhu HK, Li JK, Railkar A, Heimbrook D, Niu H (2010) Preclinical in vivo evaluation of efficacy, pharmacokinetics, and pharmacodynamics of a novel MEK1/2 kinase inhibitor RO5068760 in multiple tumor models. *Mol Cancer Ther* **9**(1): 134–144.

Davies BR, Logie A, McKay JS, Martin P, Steele S, Jenkins R, Cockerill M, Cartlidge S, Smith PD (2007) AZD6244 (ARRY-142886), a potent inhibitor of mitogen-activated protein kinase/extracellular signal-regulated kinase kinase 1/2 kinases: mechanism of action in vivo, pharmacokinetic/pharmacodynamic relationship, and potential for combination in preclinical models. *Mol Cancer Ther* **6**(8): 2209–2219.

Dudley DT, Pang L, Decker SJ, Bridges AJ, Saltiel AR (1995) A synthetic inhibitor of the mitogen-activated protein kinase cascade. *Proc Natl Acad Sci USA* **92**(17): 7686–7689.

Fremin C, Meloche S (2010) From basic research to clinical development of MEK1/2 inhibitors for cancer therapy. *J Hematol Oncol* **3**: 8.

Fujita N, Sato S, Katayama K, Tsuruo T (2002) Akt-dependent phosphorylation of p27Kip1 promotes binding to 14-3-3 and cytoplasmic localization. *J Biol Chem* **277**(32): 28706–28713.

Grunewald K, Lyons J, Frohlich A, Feichtinger H, Weger RA, Schwab G, Janssen JW, Bartram CR (1989) High frequency of Ki-ras codon 12 mutations in pancreatic adenocarcinomas. *Int J Cancer* **43**(6): 1037–1041.

Gysin S, Lee SH, Dean NM, McMahon M (2005) Pharmacologic inhibition of RAF–>MEK–>ERK signaling elicits pancreatic cancer cell cycle arrest through induced expression of p27Kip1. *Cancer Res* **65**(11): 4870–4880.

Hahn SA, Schutte M, Hoque AT, Moskaluk CA, da Costa LT, Rozenblum E, Weinstein CL, Fischer A, Yeo CJ, Hruban RH, Kern SE (1996) DPC4, a candidate tumor suppressor gene at human chromosome 18q21.1. *Science* **271**(5247): 350–353.

Hamidi H, Gustafason D, Pellegrini M, Gasson J (2011) Identification of novel targets of CSL-dependent Notch signaling in hematopoiesis. *PLoS One* **6**(5): e20022.

Hegi ME, Devereux TR, Dietrich WF, Cochran CJ, Lander ES, Foley JF, Maronpot RR, Anderson MW, Wiseman RW (1994) Allelotype analysis of mouse lung carcinomas reveals frequent allelic losses on chromosome 4 and an association between allelic imbalances on chromosome 6 and K-ras activation. *Cancer Res* **54**(23): 6257–6264.

Jones S, Zhang X, Parsons DW, Lin JC, Leary RJ, Angenendt P, Mankoo P, Carter H, Kamiyama H, Jimeno A, Hong SM, Fu B, Lin MT, Calhoun ES, Kamiyama M, Walter K, Nikolskaya T, Nikolsky Y, Hartigan J, Smith DR, Hidalgo M, Leach SD, Klein AP, Jaffee EM, Goggins M, Maitra A, Iacobuzio-Donahue C, Eshleman JR, Kern SE, Hruban RH, Karchin R, Papadopoulos N, Parmigiani G, Vogelstein B, Velculescu VE, Kinzler KW (2008) Core signaling pathways in human pancreatic cancers revealed by global genomic analyses. *Science* **321**(5897): 1801–1806.

Kamura T, Hara T, Matsumoto M, Ishida N, Okumura F, Hatakeyama S, Yoshida M, Nakayama K, Nakayama KI (2004) Cytoplasmic ubiquitin ligase KPC regulates proteolysis of p27(Kip1) at G1 phase. *Nat Cell Biol* **6**(12): 1229–1235.

Kawesha A, Ghaneh P, Andren-Sandberg A, Ograed D, Skar R, Dawiskiba S, Evans JD, Campbell F, Lemoine N, Neoptolemos JP (2000) K-ras oncogene subtype mutations are associated with survival but not expression of p53, p16(INK4A), p21(WAF-1), cyclin D1, erbB-2 and erbB-3 in resected pancreatic ductal adenocarcinoma. *Int J Cancer* **89**(6): 469–474.

Keohavong P, DeMichele MA, Melacrinos AC, Landreneau RJ, Weyant RJ, Siegfried JM (1996) Detection of K-ras mutations in lung carcinomas: relationship to prognosis. *Clin Cancer Res* **2**(2): 411–418.

Kobayashi S, Boggon TJ, Dayaram T, Jänne PA, Kocher O, Meyerson M, Johnson BE, Eck MJ, Tenen DG, Halmos B (2005) EGFR mutation and resistance of non-small-cell lung cancer to gefitinib. *N Engl J Med* **352**(8): 786–792.

Konecny GE, Winterhoff B, Kolarova T, Qi J, Manivong K, Dering J, Yang G, Chalukya M, Wang HJ, Anderson L, Kalli KR, Finn RS, Ginther C, Jones S, Velculescu VE, Riehle D, Cliby WA, Randolph S, Koehler M, Hartmann LC, Slamon DJ (2011) Expression of p16 and retinoblastoma determines response to CDK4/6 inhibition in ovarian cancer. *Clin Cancer Res* **17**(6): 1591–1602.

Lee JW, Soung YH, Kim SY, Nam HK, Park WS, Nam SW, Kim MS, Sun DI, Lee YS, Jang JJ, Lee JY, Yoo NJ, Lee SH (2005) Somatic mutations of EGFR gene in squamous cell carcinoma of the head and neck. *Clin Cancer Res* **11**(8): 2879–2882.

Li C, Wong WH (2001) Model-based analysis of oligonucleotide arrays: expression index computation and outlier detection. *Proc Natl Acad Sci USA* **98**(1): 31–36.

Little AS, Balmanno K, Sale MJ, Newman S, Dry JR, Hampson M, Edwards PA, Smith PD, Cook SJ (2011) Amplification of the driving oncogene, KRAS or BRAF, underpins acquired resistance to MEK1/2 inhibitors in colorectal cancer cells. *Sci Signal* **4**(166): ra17.

Liu X, Sun Y, Ehrlich M, Lu T, Kloog Y, Weinberg RA, Lodish HF, Henis YI (2000) Disruption of TGF-beta growth inhibition by oncogenic ras is linked to p27Kip1 mislocalization. *Oncogene* **19**(51): 5926–5935.

Medema RH, Kops GJ, Bos JL, Burgering BM (2000) AFX-like Forkhead transcription factors mediate cell-cycle regulation by Ras and PKB through p27kip1. *Nature* **404**(6779): 782–787.

Neumann J, Zeindl-Eberhart E, Kirchner T, Jung A (2009) Frequency and type of KRAS mutations in routine diagnostic analysis of metastatic colorectal cancer. *Pathol Res Pract* **205**(12): 858–862.

Nagata Y, Abe M, Motoshima K, Nakayama E, Shiku H (1990) Frequent glycine-to-aspartic acid mutations at codon 12 of c-Ki-ras gene in human pancreatic cancer in Japanese. *Jpn J Cancer Res* **81**(2): 135–140.

Peterson RT, Schreiber SL (1998) Translation control: connecting mitogens and the ribosome. *Curr Biol* **8**(7): R248–R250.

Rinehart J, Adjei AA, Lorusso PM, Waterhouse D, Hecht JR, Natale RB, Hamid O, Varterasian M, Asbury P, Kaldjian EP, Gulyas S, Mitchell DY, Herrera R, Sebolt-Leopold JS, Meyer MB (2004) Multicenter phase II study of the oral MEK inhibitor, CI-1040, in patients with advanced non-small-cell lung, breast, colon, and pancreatic cancer. *J Clin Oncol* **22**(22): 4456–4462.

Rodenhuis S, van de Wetering ML, Mooi WJ, Evers SG, van Zandwijk N, Bos JL (1987) Mutational activation of the K-ras oncogene. A possible pathogenetic factor in adenocarcinoma of the lung. *N Engl J Med* **317**(15): 929–935.

Schleger C, Verbeke C, Hildenbrand R, Zentgraf H, Bleyl U (2002) c-MYC activation in primary and metastatic ductal adenocarcinoma of the pancreas: incidence, mechanisms, and clinical significance. *Mod Pathol* **15**(4): 462–469.

Schutte M, Hruban RH, Geradts J, Maynard R, Hilgers W, Rabindran SK, Moskaluk CA, Hahn SA, Schwarte-Waldhoff I, Schmiegel W, Baylin SB, Kern SE, Herman JG (1997) Abrogation of the Rb/p16 tumor-suppressive pathway in virtually all pancreatic carcinomas. *Cancer Res* **57**(15): 3126–3130.

Sebolt-Leopold JS, Dudley DT, Herrera R, Van Becelaere K, Wiland A, Gowan RC, Tecle H, Barrett SD, Bridges A, Przybranowski S, Leopold WR, Saltiel AR (1999) Blockade of the MAP kinase pathway suppresses growth of colon tumors in vivo. *Nat Med* **5**(7): 810–816.

Shao J, Sheng H, DuBois RN, Beauchamp RD (2000) Oncogenic Ras-mediated cell growth arrest and apoptosis are associated with increased ubiquitin-dependent cyclin D1 degradation. *J Biol Chem* **275**(30): 22916–22924.

Siegel R, Ward E, Brawley O, Jemal A (2011) Cancer statistics, 2011: the impact of eliminating socioeconomic and racial disparities on premature cancer deaths. *CA Cancer J Clin* **61**(4): 212–236.

Smit VT, Boot AJ, Smits AM, Fleuren GJ, Cornelisse CJ, Bos JL (1988) KRAS codon 12 mutations occur very frequently in pancreatic adenocarcinomas. *Nucleic Acids Res* **16**(16): 7773–7782.

Span M, Moerkerk PT, De Goeij AF, Arends JW (1996) A detailed analysis of K-ras point mutations in relation to tumor progression and survival in colorectal cancer patients. *Int J Cancer* **69**(3): 241–245.

Steelman LS, Chappell WH, Abrams SL, Kempf RC, Long J, Laidler P, Mijatovic S, Maksimovic-Ivanic D, Stivala F, Mazzarino MC, Donia M, Fagone P, Malaponte G, Nicoletti F, Libra M, Milella M, Tafuri A, Bonati A, Basecke J, Cocco L, Evangelisti C, Martelli AM, Montalto G, Cervello M, McCubrey JA (2011) Roles of the Raf/MEK/ERK and PI3K/PTEN/Akt/mTOR pathways in controlling growth and sensitivity to therapy-implications for cancer and aging. *Aging (Albany NY)* **3**(3): 192–222.

Yang JY, Chang CJ, Xia W, Wang Y, Wong KK, Engelman JA, Du Y, Andreeff M, Hortobagyi GN, Hung MC (2010) Activation of FOXO3a is sufficient to reverse mitogen-activated protein/extracellular signal-regulated kinase kinase inhibitor chemoresistance in human cancer. *Cancer Res* **70**(11): 4709–4718.

Yang X, Liu S, Kharbanda S, Stone RM (2012) AKT1 induces caspase-mediated cleavage of the CDK inhibitor p27Kip1 during cell cycle progression in leukemia cells transformed by FLT3-ITD. *Leuk Res* **36**(2): 205–211.

Yip-Schneider MT, Schmidt CM (2003) MEK inhibition of pancreatic carcinoma cells by U0126 and its effect in combination with sulindac. *Pancreas* **27**(4): 337–344.